

Kinetic roughening of GaAs(001) during thermal Cl₂ etching

J. H. Schmid, A. Ballestad, B. J. Ruck,* M. Adamczyk, and T. Tiedje[†]

Department of Physics and Astronomy, University of British Columbia, Vancouver, British Columbia, V6T 1Z1 Canada

(Received 29 September 2001; revised manuscript received 11 December 2001; published 29 March 2002)

The surface morphology of Cl₂-etched GaAs(001) is measured as a function of etch time by atomic force microscopy and elastic light scattering. A flat surface is found to become rougher during the etch whereas a textured substrate becomes smoother. We have numerically simulated this behavior. It is found that the evolution of surface roughness at length scales between 50 nm and 5 μm can be described with excellent accuracy by a continuum equation for the surface height $h(\vec{x}, t)$, which is given by $dh/dt = \nu \nabla^2 h - \lambda/2(\nabla h)^2 - K \nabla^4 h + \eta$, where η is a random noise input.

DOI: 10.1103/PhysRevB.65.155315

PACS number(s): 68.55.-a, 81.15.Aa, 81.65.Cf

Typical processes in nanofabrication involve the patterning of surfaces by various etching techniques, and deposition or regrowth of thin films on these patterned substrates to create three-dimensional nanostructures. In the etching process, atoms on the surface chemically react and form volatile etch products. The chemical reactions and the removal of the etch products from the surface are inherently random processes, which are subject to fluctuations on the atomic scale. Surface roughness at mesoscopic length scales created by these fluctuations sets an ultimate limit to the precision with which nanostructures can be fabricated by chemical etching processes. It is, therefore, of great fundamental and practical importance to gain a quantitative understanding of this process.

The reaction of GaAs(001) with molecular chlorine is one of the most widely studied and employed etching processes. In recent years, much progress has been made in understanding the adsorption of halogens on semiconductor surfaces and in identifying the main reactions that are taking place on the surface.¹⁻⁴ In contrast, little is known about the evolution of surface roughness during the etch. It was found early on by optical microscopy that the thermal chlorine etch leads to a smooth surface at a substrate temperature of 300 °C, but at a lower (150 °C) or higher temperature (500 °C) the substrate becomes rough⁵. Scanning tunneling microscopy studies of GaAs(110) surfaces show that halogen etching proceeds by formation of one layer deep etch patches.⁶ In this work, we report a quantitative description of the etched surface morphology using a continuum etch equation. In this approach, the discrete nature of the atoms on the surface is averaged out and the surface height is taken to be a continuous function $h(\vec{x}, t)$ whose time rate of change can be related to various spatial derivatives of h . Possible terms that can be included in a continuum equation have been derived within the framework of kinetic roughening theory.⁷⁻⁹ Generally, in the limit of long times and large length scales, these equations lead to surfaces with characteristic scaling properties, and most experimental studies to date have concentrated on determining the relevant scaling coefficients for a given system. However, a sufficiently wide range of time and length scales to obtain reliable scaling exponents is often not accessible experimentally. In this work we demonstrate that the comparison of numerical simulations of the continuum equa-

tions with the experimental data provides a comprehensive test of the theory even in cases where reliable scaling coefficients cannot be obtained experimentally. An especially useful measure for this comparison is the power spectral density (PSD), which is defined as the square of the Fourier transform of h . We remark that the scaling properties of the particular equation used in this work depend sensitively on various saturation and crossover times and length scales.¹⁰ To obtain accurate measurements of the predicted scaling behavior one would need an experiment that spans five orders of magnitude in interface width and more than 20 orders of magnitude in time.¹⁰

Etching experiments were carried out in a UHV etch chamber attached to a V80H molecular-beam epitaxy (MBE) system. Thermal Cl₂ etching was performed at a substrate temperature of 200 °C measured with a thermocouple wire on the heater, which was originally calibrated by optical band-gap thermometry¹¹ to read the actual sample temperature. The etch chamber has a base pressure of 5×10^{-9} Torr and etching was performed at a partial Cl₂ pressure of 1×10^{-4} Torr. Under these conditions the etch rate is known to be limited by the Cl₂ flux incident on the sample,⁵ and the surface remains visually smooth during the etch. To obtain smooth starting surfaces that are free of contaminants, thin GaAs films were grown by solid source MBE at a substrate temperature of 550 °C under an As₂ overpressure. Prior to growth the native oxide was removed using an atomic hydrogen etch. The surface morphology of these grown films is known to be very smooth (≈ 0.2 nm rms roughness).¹² After growth the samples were transferred under UHV into the etch chamber without intermediate exposure to air. Surface roughness was measured by tapping mode atomic force microscopy (AFM) after removing the samples from the vacuum system. The radius of the AFM tip is about 30 nm, which tends to round off the smallest surface features. Therefore the PSD is cut off at spatial frequencies greater than about $150 \mu\text{m}^{-1}$, where tip effects may become important.

In Fig. 1 we show the PSDs as a function of spatial frequency for etch times of 1 min and 30 min obtained from a series of different sized AFM scans of each sample. We calculate the PSD in the [110] and $[1\bar{1}0]$ crystal directions and then plot the average of the two directions since there is no visible anisotropy of the surface morphology. After 1 min of

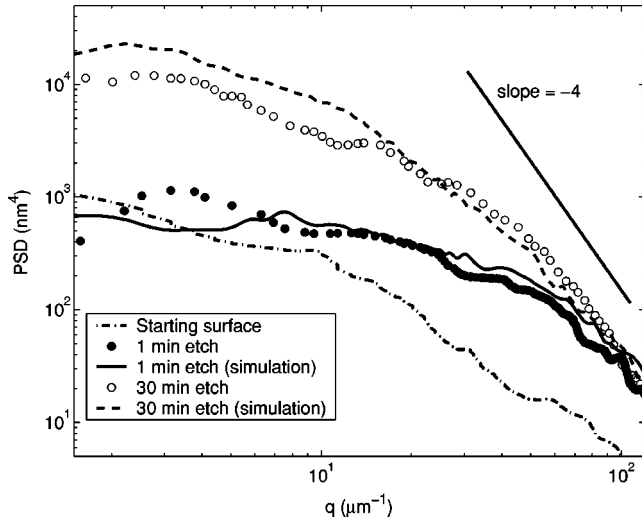


FIG. 1. PSDs of GaAs surfaces after 1 min and 30 min of etching compared to simulations based on Eq. (1) using the parameters given in the text. The PSD of the starting surface is also shown.

etching, the surface has become significantly rougher on short length scales but has hardly changed for spatial frequencies smaller than about $10 \mu\text{m}^{-1}$. After 30 min of etching, the sample is much rougher at large length scales whereas for spatial frequencies of more than $80 \mu\text{m}^{-1}$ the PSD has remained unchanged. We note that the limiting slope at large spatial frequencies of the PSD on a log-log plot is close to -4 . This behavior is expected for a fourth-order linear continuum equation.⁷ At lower spatial frequencies the PSD exhibits a rounded shape with a lower slope. This suggests that the surface evolution can be described by an equation of the form

$$\frac{\partial h}{\partial t} = \nu \nabla^2 h - \frac{\lambda}{2} (\nabla h)^2 - K \nabla^4 h + \eta, \quad (1)$$

where $\eta(\vec{x}, t)$ is a noise input that represents fluctuations of the surface height due to random processes present during the etch. PSDs of simulations, based on a numerical solution of this equation using AFM images of the grown thin film as a starting condition, are also shown in Fig. 1 for comparison. The parameters used in the simulations are $\nu = 4 \text{ nm}^2/\text{s}$, $K = 600 \text{ nm}^4/\text{s}$, and $\lambda = 1 \text{ nm/s}$.

The agreement with experiment is excellent over the entire range of spatial frequencies probed by the AFM. Note that we have used λ equal to the etch rate, which is expected theoretically if the etch propagates along the local surface normal. There is, however, no clear indication for the presence of the nonlinearity from either the AFM images or the PSDs obtained from them, as setting $\lambda = 0$ does not significantly change the results of the simulations. This is expected as even the surface that was etched for 30 min has a rms roughness of only $\approx 0.8 \text{ nm}$, while the nonlinearity is expected to play a dominant role only for a rms roughness larger than $2\nu/\lambda = 8 \text{ nm}$.¹³

Nonconservative noise is included in the simulations in the same way as described in Ref. 12. The amplitude of the

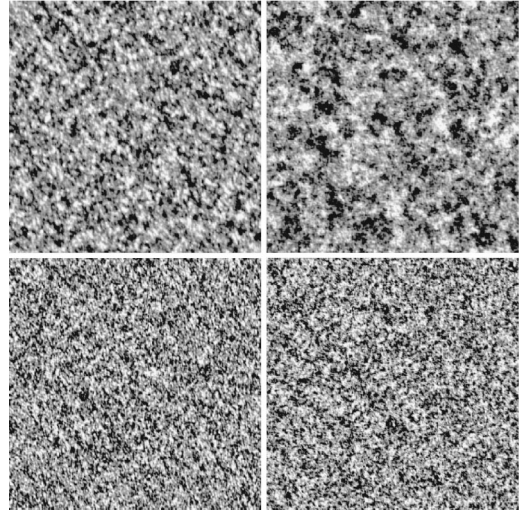


FIG. 2. Surface morphologies of GaAs thin films etched for 30 min (top) and for 1 min (bottom). AFM images (left column) are compared to simulations using Eq. (1) with the parameters given in the text (right column). The size of all images is $5 \mu\text{m} \times 5 \mu\text{m}$ and the gray scale is 1.5 nm for the top pictures and 0.7 nm for the bottom pictures.

noise added in each time step is described by a constant Γ , which we use as a fitting parameter. For noise that originates from the random removal of individual atoms during the etch, corresponding to our etch rate of 1 nm/s , $\Gamma = 1$. In our simulations we use $\Gamma = 12$, as discussed below.

On the left side of Fig. 2 we show two AFM images of surfaces after 1 min and 30 min of etching corresponding to the PSDs shown in Fig. 1. After the 1-min etch the image is dominated by short length scale roughness, which, after the longer etch time, evolves to a larger length scale corresponding to a shift in the correlation length. For the 1-min etch, the rms surface roughness caused by the atomic scale noise is about 0.8% of the etch depth. The images are compared to simulations using Eq. (1) with the parameters given above (images on the right side of Fig. 2). The simulations reproduce the dominant surface structures well. The simulation of the 30-min etch (top right) shows slightly more roughness at low spatial frequencies than the experimental AFM image (top left). This is visible both in the image and in the PSD in Fig. 1.

The model can be tested further with samples that have a different initial surface morphology, namely, the mounded surface of a GaAs thin film grown on a substrate from which the native oxide was removed by thermal desorption prior to growth rather than by an atomic H etch.¹² An AFM image of this starting surface is shown in the top part of Fig. 3. The mounds are elongated along the $[1\bar{1}0]$ crystal direction and have a height of approximately 3 nm . In the middle part of Fig. 3 we show a simulation of a 10-min-long etch with Eq. (1) using the same parameters as given above and the AFM image of the grown buffer layer as an initial condition. On short length scales the morphology of this simulated surface looks very similar to those shown in Fig. 2, but at long length scales the remnants of the mounds are still clearly visible after the etch. The experiment confirms this predic-

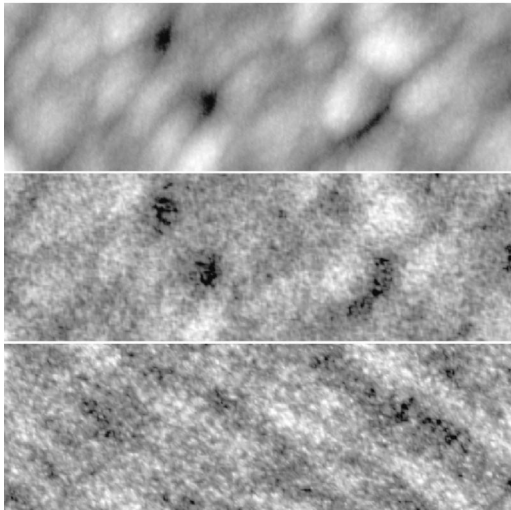


FIG. 3. AFM image of the mounded surface of a GaAs thin film (top), and a simulation of a 10-min-long etch with Eq. (1) using the AFM image above as an initial condition (middle). The same parameters were used in this simulation as in the previous ones. Bottom: An AFM image obtained from a surface etched for 10 min under the same conditions as described before but with a mounded starting surface. The size of all images is $10 \mu\text{m} \times 3.3 \mu\text{m}$ and the gray scale is 3.5 nm.

tion, as shown in the bottom part of Fig. 3, which depicts an AFM image of a surface etched for 10 min under the same conditions as before. Note that the sample orientation is different for the top and the bottom images. This explains the different direction of elongation of the mounds. The fact that the long length scale mound structure with an amplitude of $\approx 3 \text{ nm}$ remains nearly unchanged after an approximately 600-nm-deep etch is a remarkable experimental fact that has important implications for maskless pattern transfer by chemical etching processes.

To quantify the agreement between experiment and simulations, Fig. 4 shows the PSDs of the surfaces seen in Fig. 3. The mounds on the surface lead to a characteristic broad peak at low spatial frequencies ($q \lesssim 10 \mu\text{m}^{-1}$). The agreement between the experimental PSD and that obtained from the simulation is excellent. They both show that the peak originating from the mounds on the surface is not changed by the etch whereas there is significant surface roughening at high spatial frequencies ($q \gtrsim 10 \mu\text{m}^{-1}$). The power of the surface roughness at short length scales has the same q dependence as for the surfaces obtained by etching a flat initial surface. This can be seen by comparing an experimental PSD obtained in the same way as those in Fig. 1, which is shown in Fig. 4 as open circles.

We have further investigated the evolution of a randomly textured starting surface during the etch. This starting surface was obtained by a standard thermal-desorption process at a substrate temperature of $610 \text{ }^\circ\text{C}$ under an As overpressure in the MBE growth chamber. This process is known to create a surface that is randomly textured with submicron sized pits with depths of up to 30 nm.¹² An AFM scanline of this starting surface is shown in Fig. 5(a). The samples were then moved into the etch chamber where thermal Cl_2 etching was

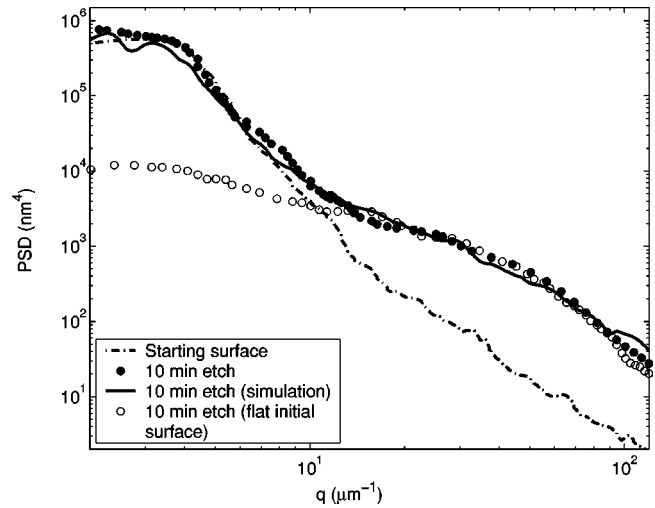


FIG. 4. Comparison of simulated and experimentally obtained PSDs of the surfaces corresponding to the images in Fig. 3. The large broad peak at low spatial frequencies corresponds to the mounds on the surface. For comparison, the open circles show the experimental PSD of a 10-min etched surface but with the smoother initial condition that is shown in Fig. 1.

performed under the same conditions as described above. It is found that the pits on the surface become wider and shallower during the etch, which can be seen in Fig. 5(c). This is consistent with the behavior expected from the linear smoothing terms in Eq. (1). In fact, a good fit to the surface profile can be obtained with the same parameters as used for the flat starting surface, as shown in Fig. 5(b). Note that the AFM scanline was used as an initial condition for the simulations whereas the scanline of the etched surface was necessarily obtained from a different sample.

The smoothing of the textured surface can also be observed by using real-time elastic light scattering (ELS). For

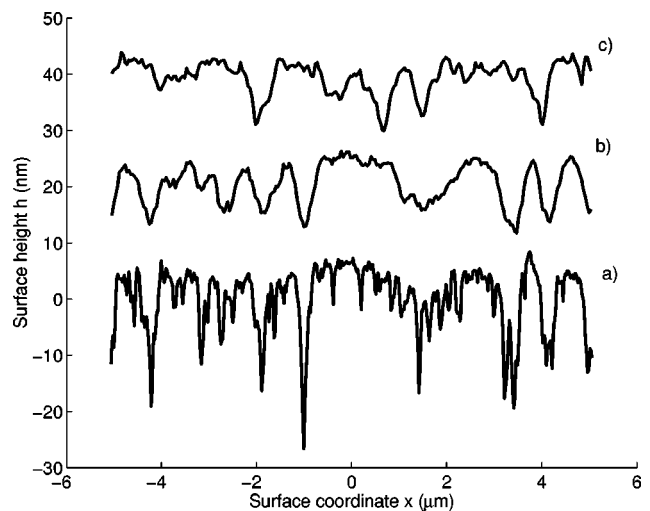


FIG. 5. (a) AFM scanline of the textured starting surface obtained by a thermal-desorption process, (b) simulations using Eq. (1) with the same parameters as before in comparison to a scanline of a surface etched for 20 min under the same conditions as described before (c). The scanlines are offset for clarity.

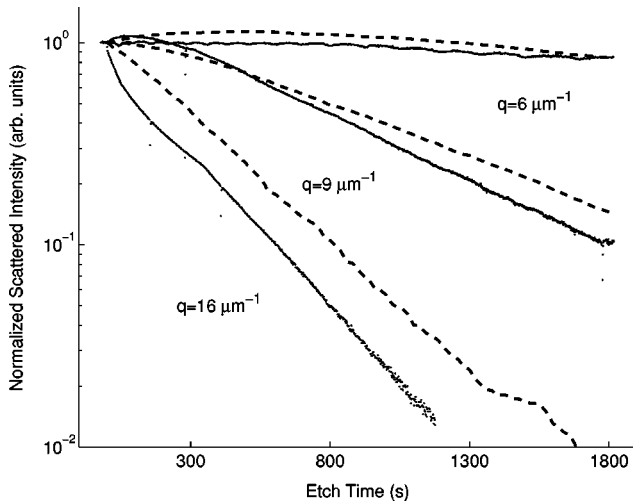


FIG. 6. Elastic light-scattering signals recorded during etching of a textured surface for three different spatial frequencies on a logarithmic scale (dotted). Results from simulations using Eq. (1) are shown as dashed lines.

these experiments, light from a He:Ne laser was incident on the sample during the etch and the diffusely scattered light from the sample surface was measured with a photomultiplier tube (PMT) fitted with a wavelength selective filter using lock-in techniques. The etch chamber has four viewports with line of sight to the sample at different angles allowing for different measurement geometries. In this way we are able to probe surface roughness at spatial frequencies q of $16 \mu\text{m}^{-1}$, $9 \mu\text{m}^{-1}$, and $6 \mu\text{m}^{-1}$. In the limit of surface roughness that is much smaller than the wavelength of the incident light (632 nm in our case), the scattered intensity measured by the PMT is directly proportional to the PSD of the surface at the spatial frequency probed.¹⁴

Results of the ELS measurements of the smoothening of the textured surface at three different spatial frequencies are shown in Fig. 6 on a logarithmic scale and compared to simulations using Eq. (1). For a purely linear etch equation, an exponential decay to the equilibrium value of the PSD with a q -dependent rate constant given by $(\nu q^2 + Kq^4)$ would be expected. Since a small amount of light scattered inside the etch chamber contributes to the measured intensity, we have subtracted a constant background from the signal. Again we have used the same parameter set to obtain an excellent fit for the initial smoothening of the pits. For these parameters the second-order linear term dominates the smoothening at the length scales probed in the ELS measurements. Clearly, the dependence of the smoothening rate on the spatial frequency is well described by this term. We also note that there is a small deviation from the purely exponential decay at the early stage of the measurements. This indicates the presence of nonlinear terms in the etch equation. The inclusion of the nonlinearity in our simulations does improve the fit to the data although the effect is quite small. The nonlinear term is more important in this case than in the roughening experiments because the initial surface rough-

ness (5 nm rms) is comparable to $2\lambda/\nu = 8$ nm. One might expect that other nonlinear or nonlocal effects not included in Eq. (1) could also be important for the evolution of a textured surface. We mention here the shadow effect,¹⁵ which, for the case of etching, leads to additional smoothening.¹⁶ This may explain the initially faster than exponential decay of the ELS signal at $16 \mu\text{m}^{-1}$, a feature that was observed quite consistently in the course of the ELS measurements.

Having identified an equation that describes the surface evolution of GaAs(001) during thermal chlorine etching, it is important to consider the physical meaning of the various terms in Eq. (1). First, the second-order linear term $\nu \nabla^2 h$ describes the effect of different desorption rates of atoms depending on a surface chemical potential that is proportional to the curvature of the surface.⁷ For the etching process, which proceeds by desorption of atoms from the surface, the presence of this term is expected. Even though we have only weak evidence for the nonlinearity $(\lambda/2)(\nabla h)^2$, as it is overshadowed by the linear terms, its presence is expected for etching that propagates along the local surface normal. The fourth-order linear term $K \nabla^4 h$ is known to arise from surface diffusion of atoms driven by a curvature dependent chemical potential.¹⁷ The exact species of molecules that are diffusing on the surface is not important for this term to be present as long as they contain Ga or As. The surface reactions in the etching process are very complex. However, for the etch conditions chosen for our measurements, it is known that the chlorination proceeds stepwise from the monochlorides to the trichlorides.¹ We believe that the diffusing species on the surface are As or Ga chlorides, although it is not known which of the chlorides are the important ones. Finally, the random noise input η corresponds to the random desorption process of atoms leaving the surface. To fit the data it was necessary to use a value for η 12 times larger than expected from the random removal of surface atoms at the etch rate. The origin of the excess noise is not known, however, the noise term in Eq. (1) increases with the size of the surface unit cell. We speculate that the excess noise is due to atomic scale correlations, namely, that the atoms are removed in patches. This is consistent with STM studies of etched surfaces.⁶

In conclusion, we have shown that the surface evolution of GaAs(001) during thermal chlorine etching can be accurately described by a simple stochastic differential equation for the surface height. In particular, we use the same equation to model quantitatively both the roughening of an initially flat surface due to atomic scale noise and the smoothening of a textured starting surface. The results provide a stringent experimental test for the kinetic roughening theory as well as new insights into the mechanism of thermal Cl_2 etching of GaAs.

We thank Richard Mar for assistance with some of the AFM scans, and NSERC and the BC Science Council (M.A.) for financial support.

- *Present address: School of Chemical and Physical Sciences, Victoria University of Wellington, Box 600, Wellington, New Zealand.
- †Also, at Department of Electrical and Computer Engineering, University of British Columbia, Vancouver, British Columbia, V6T 1Z4 Canada.
- ¹W.C. Simpson and J.A. Yarmoff, *Annu. Rev. Phys. Chem.* **47**, 527 (1996), and references therein.
- ²T. Ohno, *Phys. Rev. Lett.* **70**, 962 (1993).
- ³J.G. McLean, P. Kruse, J. Guo-Ping, H.E. Ruda, and A.C. Kummel, *Phys. Rev. Lett.* **85**, 1488 (2000).
- ⁴W.K. Wang, W.C. Simpson, and J.A. Yarmoff, *Phys. Rev. Lett.* **81**, 1465 (1998).
- ⁵N. Furuhashi, H. Miyamoto, A. Okamoto, and K. Ohata, *J. Appl. Phys.* **65**, 168 (1989).
- ⁶J.C. Patrin and J.H. Weaver, *Phys. Rev. B* **48**, 17 913 (1993).
- ⁷J. Krug, *Adv. Phys.* **46**, 139 (1997).
- ⁸A. Pimpinelli and J. Villain, *Physics of Crystal Growth* (Cambridge University Press, Cambridge, United Kingdom, 1998).
- ⁹A.-L. Barabási and H.E. Stanley, *Fractal Concepts in Surface Growth* (Cambridge University Press, Cambridge, United Kingdom, 1995).
- ¹⁰S. Majaniemi, T. Ala-Nissila, and J. Krug, *Phys. Rev. B* **53**, 8071 (1996), see Fig. 1.
- ¹¹S.R. Johnson, C. Lavoie, T. Tiedje, and J.A. Mackenzie, *J. Vac. Sci. Technol. B* **11**, 1007 (1993).
- ¹²A. Ballestad, B.J. Ruck, M. Adamczyk, T. Pinnington, and T. Tiedje, *Phys. Rev. Lett.* **86**, 2377 (2001).
- ¹³T.J. Newman and A.J. Bray, *J. Phys. A* **71**, 4299 (1996).
- ¹⁴E.L. Church, H.A. Jenkinson, and J.M. Zavada, *Opt. Eng.* **18**, 125 (1979).
- ¹⁵R.P.U. Karunasiri, R. Bruinsma, and J. Rudnick, *Phys. Rev. Lett.* **62**, 788 (1989).
- ¹⁶J.T. Drotar, Y.-P. Zhao, T.-M. Lu, and G.-C. Wang, *Phys. Rev. B* **62**, 2118 (2000).
- ¹⁷W.W. Mullins, *J. Appl. Phys.* **28**, 333 (1957).